# Improving the performance of inverted organic solar cells by adjusting the concentration of precursor solution of Al-doped ZnO*

**YU Xuan** (余璇)[1,2], **YU Xiao-ming** (于晓明)[1,2], **ZHANG Jian-jun** (张建军)[2]**, **and PAN Hong-jun** (潘洪军)[1]

*1. Innovation Application Institute, Zhejiang Ocean University, Zhoushan 316022, China*

*2. College of Electronic Information and Optical Engineering, Nankai University, Tianjin 300071, China*

(Received 5 July 2015)



Al-doped ZnO (AZO) has been used as an electron transport and hole blocking buffer layer in inverted organic solar cells (IOSCs). In this paper, the AZO morphology, optical and structural properties and IOSCs performance are investigated as a function of precursor solution concentration from 0.1 mol/L to 1.0 mol/L. We demonstrate that the device with 0.1 mol/L precursor concentration of AZO buffer layers enhances the short-circuit current and the fill factor of IOSCs simultaneously. The resulting device shows that the power conversion efficiency is improved by 35.6% relative to that of the 1.0 mol/L device, due to the improved surface morphology and transmittance (300–400 nm) of AZO buffer layer.

**Document code:** A **Article ID:** 1673-1905(2015)05-0329-4

**DOI** 10.1007/s11801-015-5127-6

Organic solar cells (OSCs) have obtained more and more attention for solar energy conversion, and they are considered as promising candidates of renewable energy resources due to the low cost, potential for commercialization large area production and fast efficiency improvement[1-4]. Al-doped ZnO (AZO) thin film, used in inverted OSCs (IOSCs) as electron transport buffer layer[5-10], is easy to be produced by a sol-gel process. The relationship between Al-doping concentration[7,8], nanostructure[10-12] of AZO and device performance has been carefully studied. However, the studies on the influence of AZO precursor solution concentration on OSCs photovoltaic performance are very limited. In this paper, we analyze the relationships between AZO characteristics, ISOC photovoltaic performance and precursor solution concentration. Devices with a structure of glass/indium tin oxide (ITO)/AZO/poly (3-hexylthiophene) (P3HT): [6, 6]-phenyl $C_{61}$ butyric acid methyl ester (PCBM)/$MoO_3$/Ag show that AZO buffer layers with Al-doping atom percent of 1% from 0.1 mol/L precursor solution enhance the short-circuit current ($J_{sc}$) and fill factor (*FF*) of IOSC device significantly, due to an improvement in the surface morphology and the increased light transmittance of AZO buffer layer.

A precursor solution consists of zinc acetate ($Zn(CH_3CO_2)_2{\cdot}2H_2O$) and aluminum nitrate ($Al(NO_3)_3{\cdot}9H_2O$) in ethanol[13]. AZO films with Al-doping atom percent of 1% were fabricated by modifying the concentration of precursor solution as 0.1 mol/L, 0.2 mol/L, 0.3 mol/L, 0.5 mol/L and 1.0 mol/L. After being spin-coated on the cleaned ITO-glass substrates, the samples were pre-annealed at 200 °C for 10 min and post annealed at 280 °C for 30 min to obtain AZO films.

The resulting AZO films were cleaned in ethanol and ultrasonic cleaned in de-ionized water for 5 min. After baking in an oven at 120 °C for 30 min, the P3HT:PCBM blend containing 20 mg/mL P3HT and 16 mg/mL PCBM in chlorobenzene was spin-coated onto the top of AZO to form an active layer (~180 nm). Finally, a 3 nm-thick $MoO_3$ film and a 70 nm-thick Ag film were thermally evaporated in sequence at $10^{-4}$ Pa through a shadow mask to form an active layer with area about 8 $mm^2$.

The morphologies of AZO films were characterized by atomic force microscopy (AFM) (Seiko SPA-400 SPM UNIT). X-ray diffraction (XRD) patterns of the films were measured by a Rigaku X-ray diffractometer (D/max-2500). The transmittance spectra were measured by a Cary spectrophotometer (Cary 5000UV–VIS). The current density-voltage (*J–V*) characteristics of IOSCs were measured with a Keithley 4200 sourcemeter under the illumination of an AM 1.5G (100 $mW{\cdot}cm^{-2}$) solar simulator.

The surface morphologies of the AZO films are shown in Fig.1, and the grain size of AZO is reduced from 9.13 nm to 9.03 nm, 7.74 nm, 7.52 nm and 7.48 nm, corresponding to the samples with the precursor solution

* This work has been supported by the National Natural Science Foundation of China (No.61377031), and the Scientific Research Foundation of Zhejiang Ocean University (No.Q1444).

** E-mail: jjzhang@nankai.edu.cn

concentrations of 1.0 mol/L, 0.5 mol/L, 0.3 mol/L, 0.2 mol/L and 0.1 mol/L, respectively. With decreasing the concentration of precursor solution from 1.0 mol/L to 0.1 mol/L, the topography tends to be more dense and homogenous, and the surface root-mean-square (*RMS*) roughness is decreases. The performance parameters of the devices with the AZO buffer layers derived from precursor solutions with different concentrations are shown in Tab.1. The dense and homogenous surface of AZO buffer layer as shown in Fig.1(e) can contribute to better contact with the active layer and facilitate charge carrier transport[14], and thus affect the device photovoltaic performance.

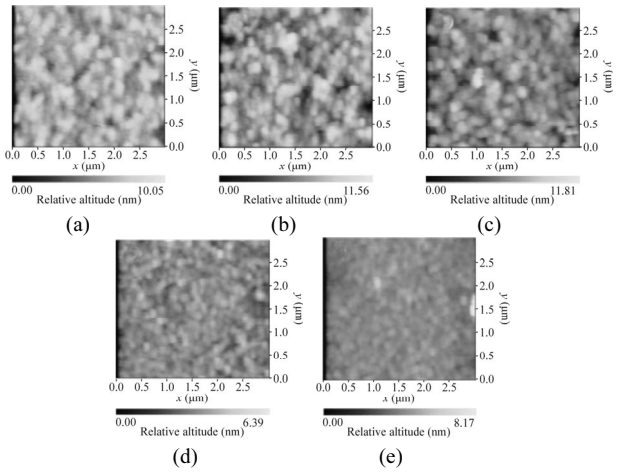


**Fig.1 AFM images of AZO films derived from precursor solutions with concentrations of (a) 1.0 mol/L, (b) 0.5 mol/L, (c) 0.3 mol/L, (d) 0.2 mol/L and (e) 0.1 mol/L**

**Tab.1 Performance parameters of the devices with the AZO buffer layers derived from precursor solutions with different concentrations**

| Concentration (mol/L) | *RMS* (nm) | Thickness (nm) | $J_{sc}$ (mA/cm$^2$) | $V_{oc}$ (V) | *FF* (%) | *PCE* (%) | $R_s$ (Ω·cm$^2$) | $R_{sh}$ (Ω·cm$^2$) |
|---|---|---|---|---|---|---|---|---|
| 1.0 | 2.05 | ~70 | 9.08 | 0.55 | 41.6 | 2.05 | 28.25 | 239.68 |
| 0.5 | 1.91 | ~45 | 9.21 | 0.57 | 42.2 | 2.14 | 26.06 | 269.66 |
| 0.3 | 1.77 | ~35 | 9.42 | 0.55 | 45.8 | 2.38 | 23.76 | 274.68 |
| 0.2 | 1.38 | ~20 | 9.54 | 0.56 | 48.8 | 2.62 | 22.76 | 301.02 |
| 0.1 | 1.13 | ~10 | 10.06 | 0.55 | 49.6 | 2.78 | 19.55 | 486.57 |

Meanwhile, the morphology and grain size play important roles in the transmittance spectra of AZO layer as shown in Fig.2. These films show an average transmittance of over 80% when the wavelength is larger than 400 nm. However, the transmittance is decreased remarkably from 300 nm to 400 nm with the increase of precursor solution concentration. The AZO film with precursor solution concentration of 1.0 mol/L (~70 nm) possesses a mean transmittance of only 59.2% from 300 nm to 400 nm. The AZO buffer layers derived from precursor solutions with different concentrations of 0.5 mol/L, 0.3 mol/L, 0.2 mol/L and 0.1 mol/L have the mean transmittances of 66.8%, 71.1%, 73.6% and 78.7% in the wavelength range from 300 nm to 400 nm, respectively. Large grain size and surface *RMS* lead to more light scatting at the interfaces and the decrease of transmittance[15]. Thus the AZO film derived from precursor solution with concentration of 0.1 mol/L with small grain size and smooth surface shows a higher transmittance than other films, especially at the wavelength from 300 nm to 400 nm, where the absorption spectrum of P3HT:PCBM active layer is located.

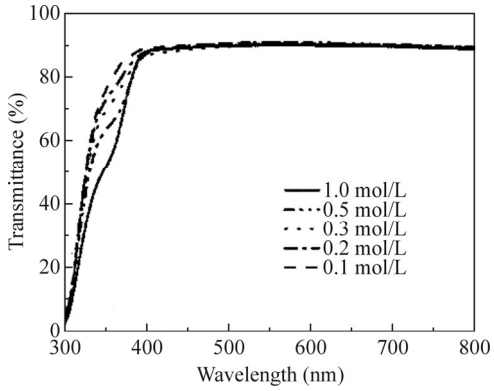


**Fig.2 The transmittance spectra of AZO layers derived from precursor solutions with different concentrations**

The XRD patterns of AZO layers are shown in Fig.3. The evident diffraction peaks of (002) of AZO films are at $2\theta$ of 34.45°, 34.33°, 34.29°, 34.17° and 34.07° with increasing precursor solution concentration from 0.1 mol/L to 1.0 mol/L. It indicates that the diffraction peak of AZO films shifts a little toward lower $2\theta$ by increasing AZO precursor solution concentration. The shift is related to the uniform state of stress with tensile components parallel to *c*-axis[16]. The relative intensity of (002) peak is very weak when the film was prepared by a single coating with thickness less than 100 nm[17]. Therefore, the average crystalline sizes and the peak intensities of all the AZO films are less than those in previous reports[18]. Also, the oriented crystal growth of AZO films can be disturbed by the substrate.

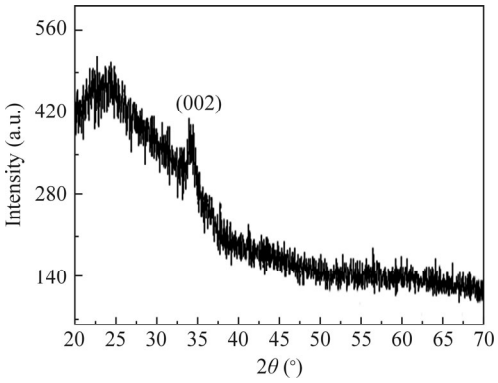

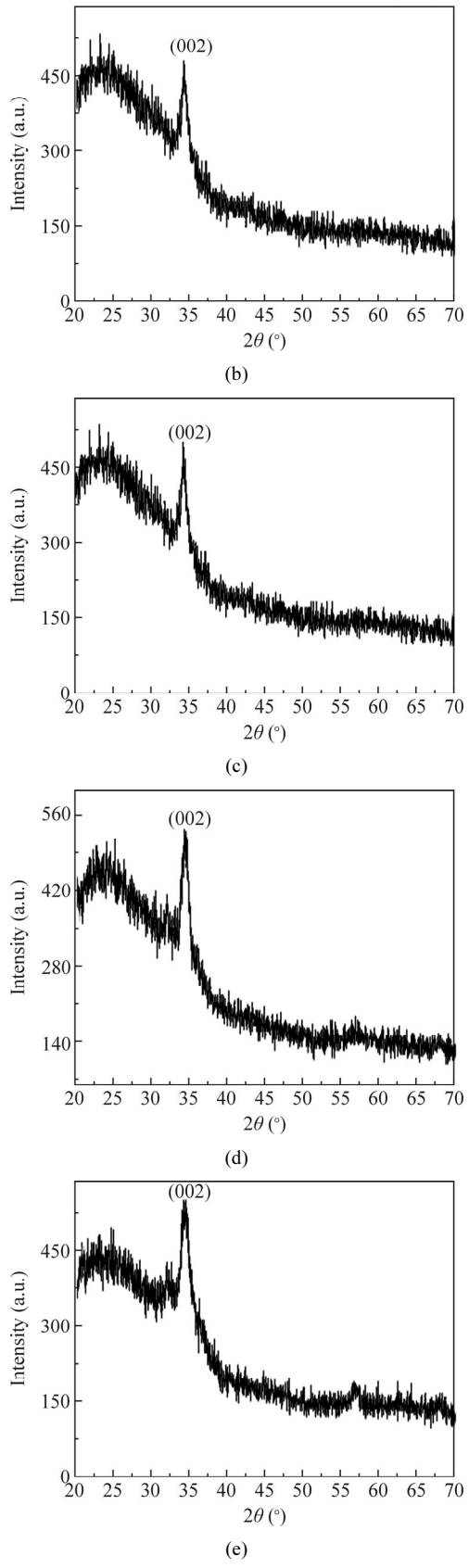


**Fig.3 XRD patterns of AZO layers derived from precursor solutions with different concentrations of (a) 0.1 mol/L, (b) 0.2 mol/L, (c) 0.3 mol/L, (d) 0.5 mol/L and (e) 1.0 mol/L**

In order to further explore the influence of AZO films on the optoelectronic performances, we investigate the *J-V* characteristics and the photoelectric conversion properties of the IOSCs as shown in Fig.4(a), and a summary of the device performance is given in Tab.1. The device with AZO buffer layer derived from precursor solution with concentration of 1.0 mol/L exhibits the $J_{sc}$ of 9.08 mA/cm$^2$, the open circuit voltage ($V_{oc}$) of 0.55 V, the *FF* of 41.6% and the power conversion efficiency (*PCE*) of 2.05%. The series resistance ($R_s$) is 28.25 Ω·cm$^2$, and the shunt resistance ($R_{sh}$) is 239.68 Ω·cm$^2$.

The device with AZO buffer layer derived from precursor solution with concentration of 0.1 mol/L exhibits a significantly increased *PCE* of 2.78%. The improvement is mainly due to the higher $J_{sc}$ and the increased *FF*. The enhanced $J_{sc}$ is attributed to the efficient light absorption, electron transport and collection associated with the smooth morphology of AZO film with precursor solution concentration of 0.1 mol/L. The AZO film with precursor solution concentration of 0.1 mol/L shows higher transmittance than other AZO films. The incident light goes through the AZO buffer layer, leads to the enhanced absorption of active layer, and is reflected in the device. The improvement is also presented in the external quantum efficiency (*EQE*) as shown in Fig.4(b).

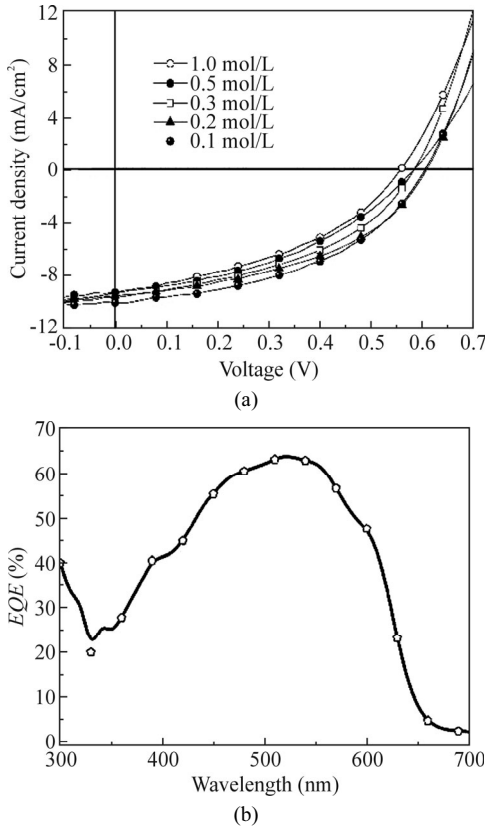


**Fig.4 (a) *J-V* characteristics of IOSCs; (b) *EQE* of the device with AZO buffer layer derived from precursor solution with concentration of 0.1 mol/L**

Meanwhile, the AZO film with precursor solution concentration of 0.1 mol/L possesses a thickness of about 10 nm, which means that the transport path of the charge carriers is shorter than those of the other AZO layers, and it is beneficial for efficient charge separation, it can reduce the carrier recombination and enhance $J_{sc}$ and $FF$[19]. Moreover, the AZO film with precursor solution concentration of 0.1 mol/L demonstrates a smooth and uniform surface morphology, which leads to a compact contact with active layer for decreasing $R_s$ (from 28.25 Ω·cm$^2$ to 19.55 Ω·cm$^2$) and increasing $R_{sh}$ (from 239.68 Ω·cm$^2$ to 486.57 Ω·cm$^2$). Therefore, the $FF$ of the device is improved simultaneously.

The effect of AZO precursor solution concentration on the performance of IOSCs is carefully studied. Compared with the AZO buffer layer derived from precursor solution with concentration of 1.0 mol/L, the 0.1 mol/L AZO (~10 nm) with an especially smooth surface exhibits efficient light transmittance, which can contribute to the enhancement of optoelectronic performance of the IOSC device. The resulting device shows that $J_{sc}$ and $FF$ can be improved simultaneously, and $PCE$ is also improved by 35.6%.

## References


[1] LIU Dong-yue, QIN Wen-jing, DONG Ni, ZHANG Qiang, YANG Lli-ying and YIN Shou-gen, Journal of Optoelectronics·Laser **25**, 1363 (2014). (in Chinese)

[2] He Z., Zhong C., Su S., Xu M., Wu H. and Cao Y., Nature Photonics **6**, 591 (2012).

[3] YU Xuan, YU Xiao-ming, HU Zi-yang, ZHANG Jian-jun, ZHAO Geng-shen and ZHAO Ying, Optoelectronics Letters **9**, 274 (2013).

[4] Zhang Q., Kan B., Liu F., Long G., Wan X., Chen X., Zuo Y., Ni W., Zhang H., Li M., Hu Z., Huang F., Cao Y., Liang Z., Zhang M., P. R. Thomas and Chen Y., Nature Photonics **9**, 35 (2015).

[5] Yu X., Yu X., Zhang J. and Zhao Y., Materials Letters **130**, 75 (2014).

[6] Thambidurai M., Kim J. Y., Song J., Ko Y., Muthukumarasamy N, Velauthapillai D and Lee C., Solar Energy **106**, 95 (2014).

[7] Chen M. H., Kuo Y. C., Lin H. H., Chao Y. P. and Wong M. S., Journal of Power Sources **275**, 274 (2015).

[8] Aprilia A., Wulandari P., Suendo V., Herman, Hidayat R., Fujii A. and Ozaki M., Solar Energy Materials & Solar Cells **111**, 181 (2013).

[9] Stubhan T., Oh H., Pinna L., Krantz J., Litzov I. and Brabec C. J., Organic Electronics **12**, 1539 (2011).

[10] Yu X., Yu X., Zhang J., Hu Z., Zhao G. and Zhao Y., Solar Energy Materials & Solar Cells **121**, 28 (2014).

[11] Lee H. Y. and Huang H. L., Organic Electronics **15**, 1362 (2014).

[12] Wolf N., Stubhan T., Manara J., Dyakonov V. and Brabec C. J., Thin Solid Films **564**, 213 (2014).

[13] Verbakel F., Meskers S. C. J. and Janssen R. A. J., Journal of Applied Physics **102**, 083701 (2007).

[14] Liang Z., Zhang Q., Wiranwetchayan O., Xi J., Yang Z., Park K., Li C. and Cao G., Advanced Functional Materials **22**, 2194 (2012).

[15] Saleem M., Fang L., Huang Q. L., Li D. C., Wu F., Ruan H. B. and Kong C. Y., Surface Review and Letters **19**, 1250055 (2012).

[16] Hong R., Shao J., He H. and Fan Z., Applied Surface Science **252**, 2888 (2006).

[17] Ohyama M., Kouzuka H. and Yoko T., Thin solid films **306**, 78 (1997).

[18] Ohyama M., Kouzuka H. and Yoko T., Journal of the American Ceramic Society **81**, 1622 (1998).

[19] Ma W., Yang C., Gong X., Lee K. and Heeger A. J., Advanced Functional Materials **15**, 1617 (2005).